

1 **Assessing the nonlinear response of fine particles to**
2 **precursor emissions: development and application of an**
3 **Extended Response Surface Modeling technique (ERSM**
4 **v1.0)**

5 **B. Zhao¹, S. X. Wang^{1,2}, K. Fu¹, J. Xing³, J. S. Fu⁴, C. Jang³, Y. Zhu⁵, X. Y. Dong⁴,**
6 **Y. Gao^{4,6}, W. J. Wu¹, J. M. Hao^{1,2}**

7 [1] State Key Joint Laboratory of Environment Simulation and Pollution Control, School of
8 Environment, Tsinghua University, Beijing 100084, China

9 [2] State Environmental Protection Key Laboratory of Sources and Control of Air Pollution
10 Complex, Beijing 100084, China

11 [3] U.S. Environmental Protection Agency, Research Triangle Park, North Carolina 27711,
12 United States

13 [4] Department of Civil and Environmental Engineering, University of Tennessee, Knoxville,
14 Tennessee 37996, United States

15 [5] School of Environmental Science and Engineering, South China University of Technology,
16 Guangzhou 510006, China

17 [6] Atmospheric Science and Global Change Division, Pacific Northwest National Laboratory,
18 Richland, Washington, 99352, United States

19 Correspondence to: S. X. Wang (shxwang@tsinghua.edu.cn)

20
21 **Abstract.**

22 An innovative Extended Response Surface Modeling technique (ERSM v1.0) is developed to
23 characterize the nonlinear response of fine particles (PM_{2.5}) to large and simultaneous changes
24 of multiple precursor emissions from multiple regions and sectors. The ERSM technique is
25 developed starting from the conventional Response Surface Modeling (RSM) technique; it
26 first quantifies the relationship between PM_{2.5} concentrations and the emissions of gaseous
27 precursors from each single region using the conventional RSM technique, and then assesses
28 the effects of inter-regional transport of PM_{2.5} and its gaseous precursors on PM_{2.5}
29 concentrations in the target region. We apply this novel technique with a widely used regional
30 chemical transport model over the Yangtze River Delta (YRD) region of China, and evaluate

1 the response of $PM_{2.5}$ and its inorganic components to the emissions of 36
2 pollutant-region-sector combinations. The predicted $PM_{2.5}$ concentrations agree well with
3 independent chemical transport model simulations; the correlation coefficients are larger than
4 0.98 and 0.99, and the mean normalized errors are less than 1% and 2% for January and
5 August, respectively. It is also demonstrated that the ERSM technique could reproduce fairly
6 well the response of $PM_{2.5}$ to continuous changes of precursor emission levels between zero
7 and 150%. Employing this new technique, we identify the major sources contributing to $PM_{2.5}$
8 and its inorganic components in the YRD region. The nonlinearity in the response of $PM_{2.5}$ to
9 emission changes is characterized and the underlying chemical processes are illustrated.

11 **1 Introduction**

12 Fine particles (i.e., particulate matter less than or equal to $2.5 \mu m$ ($PM_{2.5}$)) worsen the
13 visibility (Zhang et al., 2012), pose serious health risks (Nel, 2005) and affect the Earth's
14 climate significantly (Stocker et al., 2013). For developing countries like China and India, the
15 attainment of stringent ambient $PM_{2.5}$ standards requires large reductions of both primary
16 particles and gaseous precursors (Wang and Hao, 2012). Cost-effective control policies need
17 to consider the impact of emission reductions of multiple pollutants from multiple regions and
18 sectors, and over a wide range of stringency levels. Therefore, it is strategically important to
19 assess the response of $PM_{2.5}$ to its precursor emissions from multiple sources, which is
20 typically nonlinear owing to complex chemical mechanisms.

21 Chemical Transport Models (CTMs) are the only viable tools for evaluating the response of
22 atmospheric concentrations to different control measures (Hakami et al., 2003). The most
23 widely used technique to evaluate these responses is sensitivity analysis, i.e., the computation
24 of derivatives of modeled concentrations with respect to emission rates. "Brute force" method
25 (Russell et al., 1995; Zhang et al., 2009b; Zhao et al., 2013c; Dong et al., 2014), the most
26 frequently used method for sensitivity analysis, involves one-at-a-time variable perturbation
27 and repeated solution of the model. It is straightforward but becomes inefficient for
28 decision-making when cost-effective emission controls need to optimize over various
29 pollutants from multiple sources. A number of mathematic techniques embedded in CTMs
30 have been developed to simultaneously calculate the sensitivities of the modeled
31 concentrations to multiple variables, including the Green Function Method (GFM) and its
32 variations (Hwang et al., 1978), Automatic Differentiation in FORtran (ADIFOR, Carmichael

1 et al., 1997), Direct Method (Dickerson et al., 1982), Decoupled Direct Method (DDM, Yang
2 et al., 1997), and Adjoint Sensitivity Analysis (Sandu et al., 2005; Hakami et al., 2006). These
3 methods are used for the calculation of first-order sensitivities, and are therefore not
4 applicable for large emission changes since the nonlinearity in atmospheric responses is not
5 captured by first-order sensitivities. Improved techniques incorporating second or
6 higher-order sensitivity analysis, e.g., High-order Decoupled Direct Method (HDDM, Hakami
7 et al., 2003), and Discrete Second Order Adjoints (Sandu and Zhang, 2008), are capable of
8 capturing the nonlinearity for a perturbation of the emissions of the base case. But as methods
9 for local sensitivity analysis, they are theoretically not reliable for predicting the response of
10 atmospheric concentrations to considerably large (e.g., >50-60%) emission reductions
11 (Yarwood et al., 2013), which are nevertheless very common in air quality policy-making of
12 developing countries like China (Zhao et al., 2013b; Wang et al., 2014). Recent studies
13 (Yarwood et al., 2013; Simon et al., 2013) tried to run HDDM at several emission levels and
14 use piecewise function to predict the atmospheric concentrations over a large emission range,
15 but this modified method is only suitable for 2-3 variables. More importantly, this group of
16 method could hardly predict the response of atmospheric concentrations when multiple (>3)
17 variables of precursor emissions change simultaneously.

18 Another group of methods involves building the relationship between the modeled
19 concentrations and emission rates using statistical techniques. This type of method is
20 applicable for various CTMs regardless of the chemical mechanisms, is user-friendly for
21 decision-makers, and is particularly suitable for assessing the atmospheric response to large
22 emission changes. Milford et al. (1989) and Fu et al. (2006) simulated the ozone
23 concentrations for a number of non-methane volatile organic compound (NMVOC) and NO_x
24 reduction combinations, and derived a set of “EKMA-like” (EKMA, Empirical Kinetics
25 Modeling Approach) control isopleths, but this method is only suitable for 2-3 variables.
26 Some other studies (Heyes et al., 1996; Wang and Milford, 2001; Amann et al., 2007)
27 empirically established analytic equations for the relationship between atmospheric
28 concentrations and emission rates, and determined the parameters based on relatively small
29 numbers of model simulations. However, Xing (2011) indicated that the nonlinearity in
30 atmospheric responses could not be captured in metropolitan regions unless fourth or higher
31 order equations were used, which restricted the feasibility and accuracy of analytic equations.
32 The Response Surface Modeling (RSM) technique (denoted by “conventional RSM”

1 technique in the following text to distinguish from the ERSM technique developed in this
2 study), has been developed by using advanced statistical techniques to characterize the
3 relationship between model outputs and inputs in a highly economical manner. The number of
4 scenarios required to build RSM depends on the family of models chosen. Recently, the
5 conventional RSM technique has been applied to O₃ and PM_{2.5} related studies or
6 policy-making in the United States (U.S. Environmental Protection Agency, 2006a, b) and
7 China (Xing et al., 2011; Wang et al., 2011). In those applications, the relationships between
8 air pollutant concentrations and precursor emissions were established using the Maximum
9 Likelihood Estimation - Empirical Best Linear Unbiased Predictors (MLE-EBLUPs)
10 developed by Santner et al. (2003). Using this group of model, the number of model scenarios
11 required to build the RSM depends on the variable number via an equation of fourth or higher
12 order, even if the preferable sampling method and model configurations proposed by previous
13 studies (Santner et al., 2003) are used. Therefore, hundreds of thousands of model scenarios
14 are required to build the response surface for 10-15 or more variables, which is
15 computationally impossible for most three-dimensional CTMs. This proves a major limitation
16 for the conventional RSM technique. When considering the emissions of multiple pollutants
17 from multiple sectors in multiple regions, assessing the nonlinear response of PM_{2.5} to
18 emission changes presents a big challenge.

19 In response to this challenge, we developed a novel Extended Response Surface Modeling
20 technique (ERSM v1.0) in this study. Compared with the previous methods reviewed above,
21 this technique could characterize the nonlinear response of PM_{2.5} and its chemical
22 components to large and simultaneous changes of multiple precursor emissions from multiple
23 regions and sectors with a reasonable number of model scenarios. In particular, compared
24 with the conventional RSM technique, ERSM is applicable for an increased number of
25 variables and geographical regions. This technique is applied with the Community Multi-scale
26 Air Quality (CMAQ) model to evaluate the response of PM_{2.5} and its inorganic components to
27 precursor emissions over the Yangtze River Delta (YRD) region, one of the largest
28 city-clusters in China. The major sources contributing to PM_{2.5} and its inorganic components
29 in the YRD are identified and the nonlinearity in the response of PM_{2.5} to emission changes is
30 characterized.

1 **2 Methodology**

2 **2.1 Development of the ERSM Technique**

3 The ERSM technique is developed starting from the conventional RSM technique; the latter
4 characterizes the relationships between a response variable (e.g., $PM_{2.5}$ concentration) and a
5 set of control variables (i.e., emissions of particular precursors from particular sources)
6 following the procedures described in our previous paper (Xing et al., 2011). First, a number
7 of emission control scenarios are generated with the Latin Hypercube Sample (LHS) method
8 (Iman et al., 1980), a widely-used sampling method which ensures that the ensemble of
9 random samples is representative of actual variability. Then the $PM_{2.5}$ concentration for each
10 emission scenario is calculated with a regional CTM, and finally the RSM prediction system
11 is developed using a MPerK (MATLAB Parametric Empirical Kriging) program (Santner et
12 al., 2003) based on MLE-EBLUPs. The robustness of the conventional RSM technique has
13 been validated through leave-one-out cross validation, out of sample validation and 2-D
14 isopleths validation, as documented in our previous papers (Xing et al., 2011; Wang et al.,
15 2011).

16 The ERSM technique first quantifies the relationship between $PM_{2.5}$ concentrations and the
17 emissions of gaseous precursors from each single region with the conventional RSM
18 technique following the procedures described in the last paragraph, and then assesses the
19 effects of inter-regional transport of $PM_{2.5}$ and its gaseous precursors on $PM_{2.5}$ concentration
20 in the target region. In order to quantify the interaction among regions, we make a key
21 assumption that the emissions of gaseous precursors in the source region affect $PM_{2.5}$
22 concentrations in the target region through two major processes: (1) the inter-regional
23 transport of gaseous precursors enhancing the chemical formation of secondary $PM_{2.5}$ in the
24 target region; (2) the formation of secondary $PM_{2.5}$ in the source region followed by transport
25 to the target region. We quantify the contribution of these two processes to the interactions
26 between any two regions, and assess the inter-regional influences among multiple regions by
27 integrating the contributions of each process. Then, a particular approach was implemented to
28 improve the accuracy of the response surface when the gaseous emissions from multiple
29 regions experience quite large reductions simultaneously.

30 Finally, $PM_{2.5}$ concentrations are linearly dependent on primary $PM_{2.5}$ emissions, therefore we
31 predict the changes of $PM_{2.5}$ concentrations owing to the changes of primary $PM_{2.5}$ emissions

1 by simply interpolating between the base case and a sensitivity scenario where one control
2 variable of primary $PM_{2.5}$ is disturbed and the other variables stay constant.

3 Since the method to develop the relationship between $PM_{2.5}$ concentrations and primary $PM_{2.5}$
4 emissions is straightforward, we will focus on the response of $PM_{2.5}$ and its chemical species
5 to the emissions of gaseous precursors in the following texts. To facilitate the explanation, we
6 assume a simplified but general case which involves three regions, defined as A, B, and C,
7 and three control variables in each region, i.e., NO_x emissions of Sector 1, NO_x emissions of
8 Sector 2, and total NH_3 emissions. The response variable is $PM_{2.5}$ concentration in the urban
9 area of Region A. Although the technique is illustrated for this simplified case, it is also
10 applicable for different response variable (e.g., NO_3^- , SO_4^{2-} , and NH_4^+), and different numbers
11 of regions/pollutants/sectors. A detailed description of the ERSM technique using the
12 simplified case is given below, and a flowchart illustrating this technique is shown in Fig. 1.

13 The emission control scenarios required to build the response surface include: (1) the base
14 case; (2) N scenarios generated by applying the LHS method for the control variables in each
15 single region; and (3) M scenarios generated by applying the LHS method for the total
16 emissions of gaseous precursors (NO_x and NH_3 for this case) in all regions. The scenario
17 numbers N and M are determined in order that they are sufficient to accurately construct the
18 relationship between the response variable and randomly changing control variables.
19 Specifically, we gradually increase the scenario number and build the response surface
20 repeatedly until the prediction performance is good enough based on the results of out of
21 sample validation and 2-D isopleths validation (Xing et al., 2011; Wang et al., 2011). Based
22 on our previous studies (Xing et al., 2011; Wang et al., 2011), the response surface for 2 and 3
23 variables could be built with good prediction performance (mean normalized error < 1%;
24 correlation coefficient > 0.99) using 30 and 50 scenarios, respectively; therefore, for this
25 simplified case, N=50, and M=30. The required scenario number for the simplified case is
26 therefore 1 (the base case) + 50 (scenarios for each single region) * 3 (number of regions) +
27 30 (scenarios for the total precursor emissions in all regions) = 181.

28 Employing conventional RSM technique, we build the response surface of $PM_{2.5}$
29 concentration in Region A to the concentrations of precursors in Region A using the base case
30 and the 50 scenarios where the variables in Region A change randomly but those in other
31 regions remain constant:

$$32 \quad [PM_{2.5}]_A = [PM_{2.5}]_{A0} + RSM_{A \rightarrow A}^{PM_{2.5}}([NO_x]_A, [NH_3]_A) \quad (1)$$

1 where $[PM_{2.5}]_A$, $[NOx]_A$, and $[NH3]_A$ are the concentrations of $PM_{2.5}$, NOx and NH_3 in
 2 Region A, respectively. $[PM_{2.5}]_{A0}$ is the $PM_{2.5}$ concentration in Region A in the base case.
 3 RSM represents the response surface we build with conventional RSM technique; the
 4 superscript (“ $PM_{2.5}$ ” in this case) represents the response variable; the letters before and after
 5 the arrow in the subscript (both are “A” in this case) represent the source and receptor regions,
 6 respectively. Further, we develop the relationship between precursor concentrations and the
 7 changes of precursor emissions in Region A with the same 51 scenarios (we use NOx
 8 concentration as example, and it is equivalent for NH_3):

$$9 \quad [NOx]_{A \rightarrow A} = RSM_{A \rightarrow A}^{NOx} (Emis_NOx_1_A, Emis_NOx_2_A, Emis_NH3_A) \quad (2)$$

10 where $Emis_NOx_1_A$, $Emis_NOx_2_A$, and $Emis_NH3_A$ are NOx emissions of Sector 1, NOx
 11 emissions of Sector 2, and total NH_3 emissions in Region A, respectively. $[NOx]_{A \rightarrow A}$,
 12 representing the changes of NOx concentration in Region A compared with the base case in
 13 response to the emission changes in the same region, is defined as

$$14 \quad [NOx]_{A \rightarrow A} = [NOx]_A - [NOx]_{A0} \quad (3)$$

15 where $[NOx]_{A0}$ is the NOx concentration in Region A in the base case.

16 Following similar procedures, the response of the concentrations of $PM_{2.5}$ and its gaseous
 17 precursors in Region A to the changes of precursor emissions in Region B (the same method
 18 applies for Region C) can be developed using the base case and the 50 scenarios where the
 19 variables in Region B change randomly but those in other regions remain constant:

$$20 \quad [PM_{2.5}]_{B \rightarrow A} = RSM_{B \rightarrow A}^{PM_{2.5}} (Emis_NOx_1_B, Emis_NOx_2_B, Emis_NH3_B) \quad (4)$$

$$21 \quad [NOx]_{B \rightarrow A} = RSM_{B \rightarrow A}^{NOx} (Emis_NOx_1_B, Emis_NOx_2_B, Emis_NH3_B) \quad (5)$$

$$22 \quad [NH3]_{B \rightarrow A} = RSM_{B \rightarrow A}^{NH3} (Emis_NOx_1_B, Emis_NOx_2_B, Emis_NH3_B) \quad (6)$$

23 where $[PM_{2.5}]_{B \rightarrow A}$, $[NOx]_{B \rightarrow A}$, and $[NH3]_{B \rightarrow A}$ are the changes of $PM_{2.5}$, NOx , and NH_3
 24 concentrations in Region A compared with the base case in response to the emission changes
 25 in Region B. $Emis_NOx_1_B$, $Emis_NOx_2_B$, and $Emis_NH3_B$ are NOx emissions of Sector
 26 1, NOx emissions of Sector 2, and total NH_3 emissions in Region B, respectively.

27 As described above, the influence of gaseous precursor emissions in Region B on $PM_{2.5}$
 28 concentration in Region A, as expressed by Eq. (4), can be broken down into two major
 29 processes: (1) the transport of gaseous precursors from Region B to Region A that enhances
 30 the chemical formation of secondary $PM_{2.5}$ in Region A; (2) the formation of secondary $PM_{2.5}$
 31 in Region B followed by transport to Region A. In order to quantify the contribution of the

1 first process, we firstly use Eq. (5) and Eq. (6) to quantify the effect of the transport of
 2 gaseous precursors from Region B to Region A on the precursor concentrations in Region A.
 3 How much does the change of precursor concentrations in Region A enhance the chemical
 4 formation of secondary PM_{2.5} in Region A? To answer this question, we introduce a
 5 straightforward assumption that the changes of PM_{2.5} concentration owing to changes of
 6 precursor concentrations in the same region (described by Eq. (1)) are solely attributable to
 7 changes of local chemical formation. Strictly speaking, the changes of precursor concentration
 8 in Region A might affect the precursor concentrations/PM_{2.5} concentrations in other regions,
 9 which might in turn affect the PM_{2.5} concentrations in Region A; but this “indirect” pathway
 10 is thought to be negligible in this study. Based on this assumption, the contribution of the first
 11 process to PM_{2.5} concentrations in Region A is expressed as

$$12 \quad [PM_{2.5_Chem}]_{B \rightarrow A} = RSM_{A \rightarrow A}^{PM_{2.5}} ([NOx]_{A0} + [NOx]_{B \rightarrow A}, [NH3]_{A0} + [NH3]_{B \rightarrow A}) \quad (7)$$

13 where $[PM_{2.5_Chem}]_{B \rightarrow A}$ is the change of PM_{2.5} concentration in Region A affected by the
 14 changes of precursor emissions in Region B through the inter-regional transport of gaseous
 15 precursors (the first process). The contribution of the second process to PM_{2.5} concentration in
 16 Region A (denoted by $[PM_{2.5_Trans}]_{B \rightarrow A}$ defined below) is then calculated by extracting the
 17 contribution of the first process (Eq. (7)) from the total (Eq. (4)), as expressed by Eq. (8).

$$18 \quad [PM_{2.5_Trans}]_{B \rightarrow A} = [PM_{2.5}]_{B \rightarrow A} - [PM_{2.5_Chem}]_{B \rightarrow A} \quad (8)$$

19 where $[PM_{2.5_Trans}]_{B \rightarrow A}$ is the change of PM_{2.5} concentration in Region A affected by the
 20 changes of precursor emissions in Region B through the transport of secondary PM_{2.5} (the
 21 second process).

22 We also need to know the relationship between $[PM_{2.5_Trans}]_{B \rightarrow A}$ and the precursor
 23 emissions in Region B. Therefore, we quantify this relationship using conventional RSM
 24 technique, as described by Eq. (9).

$$25 \quad [PM_{2.5_Trans}]_{B \rightarrow A} = RSM_{B \rightarrow A}^{PM_{2.5_Trans}} (Emis_NOx_1_B, Emis_NOx_2_B, Emis_NH3_B) \quad (9)$$

26 For the emission scenario whose PM_{2.5} concentration is to be predicted, we presume that its
 27 emissions of gaseous precursors in all the three regions are arbitrary. In this case, the change
 28 of PM_{2.5} is expressed as an integrated effect of the changes of local precursor emissions, the
 29 inter-regional transport of precursors enhancing local chemical reactions, and the
 30 inter-regional transport of secondary PM_{2.5}:

$$31 \quad [PM_{2.5}]_A = [PM_{2.5}]_{A0} + RSM_{A \rightarrow A}^{PM_{2.5}} ([NOx]_{A0} + [NOx]_{A \rightarrow A} + [NOx]_{B \rightarrow A} + [NOx]_{C \rightarrow A},$$

$$32 \quad [NH3]_{A0} + [NH3]_{A \rightarrow A} + [NH3]_{B \rightarrow A} + [NH3]_{C \rightarrow A}) + [PM_{2.5_Trans}]_{B \rightarrow A} + [PM_{2.5_Trans}]_{C \rightarrow A} \quad (10)$$

1 where $[PM_{2.5_Trans}]_{B \rightarrow A}$ is calculated using Eq. (9), and $[PM_{2.5_Trans}]_{C \rightarrow A}$ is calculated
 2 using an equivalent equation for which the independent variables are the gaseous emissions in
 3 Region C. It should be noted that $[PM_{2.5_Trans}]_{B \rightarrow A}$ cannot be calculated using Eq. (8)
 4 because Eq. (8) holds only if the emissions in the regions other than Region B remain at the
 5 base-case levels.

6 Strictly speaking, $[PM_{2.5_Trans}]_{B \rightarrow A}$ and $[PM_{2.5_Trans}]_{C \rightarrow A}$ could interact with each other.
 7 In other words, the changes of precursor emissions in Region C might affect the formation of
 8 secondary $PM_{2.5}$ in Region B, which further affects the transport of secondary $PM_{2.5}$ from
 9 Region B to Region A. Eq. (9) and Eq. (10) implies an assumption that $[PM_{2.5_Trans}]_{B \rightarrow A}$
 10 depends only on the precursor emissions in Region B, and is independent of precursor
 11 emissions in other regions. That is, the interaction between $[PM_{2.5_Trans}]_{B \rightarrow A}$ and
 12 $[PM_{2.5_Trans}]_{C \rightarrow A}$ is neglected.

13 It should be noted that Eq. (1), which relates the changes of $PM_{2.5}$ concentration in Region A
 14 (equivalent to the changes of local chemical formation of $PM_{2.5}$ as discussed above) to local
 15 precursor concentrations, is established using the base case and the 50 scenarios where the
 16 variables in Region A change randomly but those in other regions remain constant. This
 17 means Eq. (1) is only applicable for the concentration range below (we use NO_X as example,
 18 it is equivalent for NH_3)

$$19 \quad [NO_X]_A \geq [NO_X]_{A, min} = [NO_X]_{A0} + [NO_X]_{A \rightarrow A, min} = [NO_X]_{A0} + RSM_{A \rightarrow A}^{NO_X}(0, 0, 0) \quad (11)$$

20 where $[NO_X]_{A, min}$ is defined as the minimum NO_X concentration in Region A when the
 21 emissions from Region A change arbitrarily and those in other regions remain the base-case
 22 levels.

23 Eq. (10) relies on Eq. (1) but might exceed its available range, i.e., $[NO_X]_A < [NO_X]_{A, min}$, or
 24 $[NH_3]_A < [NH_3]_{A, min}$, when the precursor emissions in multiple regions are reduced
 25 considerably at the same time. In this case, we quantify the changes of $PM_{2.5}$ concentrations
 26 owing to local chemical formation through a different approach. First, the local chemical
 27 formation of $PM_{2.5}$ can be tracked easily in widely-used three-dimensional CTMs. For
 28 example, a module named “process analysis” has already been implemented in CMAQ, which
 29 outputs the contribution of major physical and chemical processes to air pollutant
 30 concentrations. The chemical formation of $PM_{2.5}$ in Region A is estimated as

$$31 \quad Prod_PM_A = AERO_PM_A + CLDS_PM_A \quad (12)$$

1 where $AERO_PM_A$ and $CLDS_PM_A$ are the contribution of aerosol process and in-cloud
 2 process to $PM_{2.5}$ concentration in Region A, extracted from CMAQ using the module
 3 “process analysis”. When the ERSM technique is applied with other CTMs, the chemical
 4 formation of $PM_{2.5}$ can be readily extracted in a similar way. In addition, the chemical
 5 formation of $PM_{2.5}$ in Region A and the resulting $PM_{2.5}$ concentrations present a linear
 6 relationship, which can be established using the base case and the 50 scenarios where the
 7 variables in Region A change randomly but those in other regions remain constant:

$$8 \quad [PM_{2.5}]_A = k \cdot Prod_PM_A + b \quad (13)$$

9 where k and b are parameters decided through regression, and the correlation coefficient is
 10 approximately 0.99. Then we develop the relationship between the local chemical formation
 11 of $PM_{2.5}$ in Region A and local precursor concentrations using the base case and the 30
 12 scenarios where control variables in all regions change together and the variables for the same
 13 pollutant (e.g., $Emis_NH3_A$, $Emis_NH3_B$, and $Emis_NH3_C$) equal each other:

$$14 \quad Prod_PM_A = RSM_{A \rightarrow A}^{Prod_PM}([NOx]_A, [NH3]_A) \quad (14)$$

15 Combining Eq. (13) and Eq. (14), and considering the effect of inter-regional transport of
 16 $PM_{2.5}$ (calculated using Eq. (9)), we derive

$$17 \quad [PM_{2.5}]_A = k \cdot RSM_{A \rightarrow A}^{Prod_PM}([NOx]_{A0} + [NOx]_{A \rightarrow A} + [NOx]_{B \rightarrow A} + [NOx]_{C \rightarrow A},$$

$$18 \quad [NH3]_{A0} + [NH3]_{A \rightarrow A} + [NH3]_{B \rightarrow A} + [NH3]_{C \rightarrow A}) + b + [PM_{2.5_Trans}]_{B \rightarrow A} + [PM_{2.5_Trans}]_{C \rightarrow A}$$

$$19 \quad (\text{applicable for } [NOx]_A < [NOx]_{A, min}, \text{ or } [NH3]_A < [NH3]_{A, min}) \quad (15)$$

19 It should be noted that the “process analysis” module could also be used within the first
 20 approach (Eq. (10)) to distinguish the contributions of chemical formation and physical
 21 transport. However, in the first approach, we could distinguish the chemical and transport
 22 contributions even without this diagnostic module (see Eq. (7) and Eq. (8)). If this module
 23 was used, we would need to develop the relationship between the chemically formed $PM_{2.5}$
 24 and the $PM_{2.5}$ concentration, which was an extra step compared with the first approach and
 25 added to the complexity.

26 To assure the consistency between Eq. (10) and Eq. (15), we introduce “transition intervals”
 27 of $([NOx]_{A, min}, [NOx]_{A, min} + \delta_{NOx})$ and $([NH3]_{A, min}, [NH3]_{A, min} + \delta_{NH3})$, where
 28 $\delta_{NOx} = 0.1 * [NOx]_{A0}$ and $\delta_{NH3} = 0.1 * [NH3]_{A0}$. Eq. (10) is applied for
 29 $[NOx]_A \geq [NOx]_{A, min} + \delta_{NOx}$ and $[NH3]_A \geq [NH3]_{A, min} + \delta_{NH3}$, and we linearly interpolate
 30 between Eq. (10) and Eq. (15) for the transitional range. Based on the case study in the YRD

1 region (see Sect. 2.2), the discrepancy between the two approaches is 1-8% in the transition
2 interval.

3 **2.2 Case study of the YRD region**

4 The ERSM technique was applied with CMAQ version 4.7.1 over the YRD region of China.
5 One-way, triple nesting simulation domains are used, as shown in Fig. 2. Domain 1 covers
6 most of China and part of East Asia with a grid resolution of 36 km×36 km; domain 2 covers
7 the eastern China with a grid resolution of 12 km×12 km; domain 3 covers the Yangtze River
8 Delta region with a grid resolution of 4 km×4 km. The Weather Research and Forecasting
9 Model (WRF, version 3.3) was used to generate the meteorological fields. The physical and
10 chemical options of CMAQ and WRF, the geographical projection, the vertical resolution,
11 and the initial and boundary conditions are consistent with our previous papers (Zhao et al.,
12 2013a, c). A high-resolution anthropogenic emission inventory for the YRD region developed
13 by Fu et al. (2013) was used. The anthropogenic emissions for other regions in East Asia were
14 from Zhao et al. (2013a, c) and Wang et al., (2014), and emissions for other Asian countries
15 were taken from the INDEX-B inventory (Zhang et al., 2009a). The biogenic emissions were
16 calculated by the Model of Emissions of Gases and Aerosols from Nature (MEGAN,
17 Guenther et al., 2006). The ERSM technique is applicable for various time scales, ranging
18 from a single day to several years. The simulation period for this case study is January and
19 August in 2010, representing winter and summer, respectively. One may want to extend the
20 analysis to a full year. The most rigorous way is to finish the CMAQ simulations for a full
21 year and build the response surfaces following the same procedure. Alternatively, the
22 relationship for a full year can be roughly estimated using the average values of January and
23 August. Another approach is to finish the simulations for an additional month in Spring and
24 Autumn, respectively, and represent the situation of a full year with the average values of the
25 four typical months. The simulated meteorological parameters, and concentrations of PM₁₀,
26 PM_{2.5}, and their chemical components agree fairly well with observation data, as described in
27 detail in the Supporting Information (Table S1-S2, Fig. S1-S3).

28 Domain 3 was divided into 4 regions (see Fig. 2), i.e. Shanghai, southern Jiangsu province
29 (“Jiangsu”), northern Zhejiang province (“Zhejiang”), and other regions (“Others”). We
30 developed two RSM/ERSM prediction systems (Table 1); the response variables for both of
31 them are the concentrations of PM_{2.5}, SO₄²⁻, and NO₃⁻ over the urban areas of major cities (see
32 Fig. 2) in these four regions. The first prediction system used the conventional RSM

1 technique and 101 emission control scenarios generated by the LHS method to map
2 atmospheric concentrations versus total emissions of NO_x , SO_2 , NH_3 , NMVOC, and $\text{PM}_{2.5}$ in
3 Domain 3. For the second prediction system, the emissions of gaseous $\text{PM}_{2.5}$ precursors and
4 primary $\text{PM}_{2.5}$ in each of the four regions are categorized into 6 and 3 control variables,
5 respectively (see Table 1), resulting in 36 control variables in total. Note that we did not
6 consider NMVOC emissions in the second prediction system, because the contribution of
7 NMVOC to $\text{PM}_{2.5}$ concentrations is small in the current CMAQ model, mainly due to the
8 significant underestimation of secondary organic aerosol formation (Carlton et al., 2010). We
9 generated 663 scenarios (see Table 1) to build the response surface, following the method to
10 create emission scenarios for the ERSM technique (the 5th paragraph of Sect. 2.1). In detail,
11 the scenarios include (1) 1 CMAQ base case; (2) $N=150$ scenarios generated by applying LHS
12 method for the control variables of gaseous precursors in Shanghai, 150 scenarios generated
13 in the same way for Jiangsu, 150 scenarios for Zhejiang, and 150 scenarios for Others; (3)
14 $M=50$ scenarios generated by applying LHS method for the total emissions of NO_x , SO_2 , and
15 NH_3 in all regions; and (4) 12 scenarios where one of the control variables of primary $\text{PM}_{2.5}$
16 emissions is set to 0.25 for each scenario. Here the number $N=150$ and $M=50$ are decided
17 according to the numerical experiments conducted in our previous studies (Xing et al., 2011;
18 Wang et al., 2011), which showed that the response surface for 6 and 3 variables could be
19 built with good prediction performance (mean normalized error $< 1\%$; correlation coefficient $>$
20 0.99) using 150 and 50 scenarios, respectively. Finally, we generated 40 independent
21 scenarios for out-of-sample validation, as described in detail in Sect. 3.1.

22 **3 Results and discussion**

23 **3.1 Validation of ERSM performance**

24 The performance of the conventional RSM technique has been well evaluated in our previous
25 studies (Xing et al., 2011; Wang et al., 2011). In this study we focus on the validation of the
26 ERSM technique. Using the prediction system built with the ERSM technique, we predicted
27 the $\text{PM}_{2.5}$ concentrations for 40 “out-of-sample” control scenarios, i.e., scenarios independent
28 from those used to build the ERSM prediction system, and compared with the corresponding
29 CMAQ simulations. These 40 out-of-sample scenarios include 32 cases (case 1-32) where the
30 control variables of gaseous precursors change but those of primary $\text{PM}_{2.5}$ stay the same as
31 the base case, 4 cases (case 33-36) the other way around, and 4 cases (case 37-40) where
32 control variables of gaseous precursors and primary $\text{PM}_{2.5}$ change simultaneously. Most cases

1 are generated randomly with the LHS method (case 4-6, 10-12, 16-18, 22-24, 28-40), and
 2 some cases are designed where all control variables are subject to large emission changes
 3 (case 1-3, 7-9, 13-15, 19-21, 25-27). A more detailed description of the out-of-sample control
 4 scenarios is given in Table S3. Two statistical indices, the Normalized Error (NE) and Mean
 5 Normalized Error (MNE) are defined as follows:

$$6 \quad NE = |P_i - S_i| / S_i \quad (16)$$

$$7 \quad MNE = \frac{1}{N_s} \sum_{i=1}^{N_s} [|P_i - S_i| / S_i] \quad (17)$$

8 where P_i and S_i are the ERSM-predicted and CMAQ-simulated value of the i^{th}
 9 out-of-sample scenario; N_s is the number of out-of-sample scenarios. Figure 3 compares the
 10 ERSM-predicted and CMAQ-simulated $PM_{2.5}$ concentrations for the out-of-sample scenarios
 11 using scattering plots (the raw data for the scattering plots are given in Table S4-S5). Table 2
 12 shows the statistical results for the comparison. It can be seen that the ERSM predictions and
 13 CMAQ simulations agree well with each other. The correlation coefficients are larger than
 14 0.98 and 0.99, and the MNEs are less than 1% and 2% for January and August, respectively.
 15 The maximum NEs could be as large as 6% and 10% in January and August, respectively, but
 16 the NEs for 95% of all out-of-sample scenarios fall below 3.5%. NEs exceeding 3.5% happen
 17 only for the scenario where all control variables are reduced by 90% (case 25). In addition,
 18 the maximum NEs for case 33-36 are all within 0.2%, indicating a perfect linear relationship
 19 between $PM_{2.5}$ concentrations and primary $PM_{2.5}$ emissions.

20 We further evaluated the performance of the ERSM technique by comparing the 2D-isopleths
 21 of $PM_{2.5}$ concentrations in response to the simultaneous changes of $NO_x/SO_2/NH_3$ emissions
 22 in all regions derived from both the conventional RSM and the ERSM technique. Figure 4, S4,
 23 and S5 show the isopleths of $PM_{2.5}$ concentrations in Shanghai, Jiangsu, and Zhejiang,
 24 respectively. The X- and Y-axis of the figures show the “emission ratio”, defined as the ratios
 25 of the changed emissions to the emissions in the base case. For example, an emission ratio of
 26 1.5 means the emissions of a particular control variable increase by 50% from the base case.
 27 The different colors represent different $PM_{2.5}$ concentrations. The comparison shows that the
 28 shapes of isopleths derived from both prediction systems agree fairly well with each other,
 29 although the isopleths predicted by the ERSM technique are not as smooth as those predicted
 30 by the conventional RSM technique owing to a much larger variable number. The consistency
 31 between the conventional RSM and ERSM prediction systems indicates that the ERSM
 32 technique could reproduce fairly well the response of $PM_{2.5}$ to continuous changes of

1 precursor emission levels between zero and 150%. Although model simulations definitely
2 have numerical errors, the success in capturing the atmospheric responses to continuous
3 emission changes over a full range of control levels ensures that these errors could not
4 challenge the major conclusions about the effectiveness of air pollution control measures.

5 **3.2 Response of PM_{2.5} to precursor emissions.**

6 The ERSM prediction system could instantly evaluate the response of PM_{2.5} and its chemical
7 components to the independent or simultaneous changes of the precursor emissions from
8 multiple sectors and regions, over a full range of control levels. Therefore, it improves the
9 identification of major precursors, regions, and sectors contributing to PM_{2.5} pollution. This
10 unique capability distinguishes the ERSM from the previous sensitivity analysis methods.

11 Following previous sensitivity studies, we define PM_{2.5} sensitivity as the change ratio of
12 PM_{2.5} concentration divided by the reduction ratio of emissions:

$$13 S_a^X = [(C^* - C_a) / C^*] / (1 - a) \quad (18)$$

14 where S_a^X is the PM_{2.5} sensitivity to emission source X at its emission ratio a ; C_a is the
15 concentration of PM_{2.5} when the emission ratio of X is a ; and C^* is the concentration of
16 PM_{2.5} in the base case (when emission ratio of X is 1). Figure 5 shows the PM_{2.5} sensitivity to
17 the stepped control of individual air pollutants, and Fig. 6 shows the PM_{2.5} sensitivity to the
18 stepped control of individual air pollutants from individual sectors. Figure 5 can be derived
19 from the prediction systems built with both the conventional RSM and ERSM technique,
20 except that the latter did not evaluate the effects of the changes of NMVOC emissions. The
21 results derived from both systems are consistent, and we present those derived from the
22 conventional technique to include the effects of NMVOC. Figure 6 is derived from the ERSM
23 technique.

24 In January, PM_{2.5} concentrations are sensitive to the primary PM_{2.5} emissions, followed by
25 NH₃, and relatively insensitive to NO_x and SO₂. The contribution of primary PM_{2.5} is
26 dominated by the emissions from industrial and residential sources. During August, gaseous
27 precursors make larger contributions to PM_{2.5} concentrations than primary PM_{2.5}, with similar
28 contributions from NH₃, SO₂, and NO_x. The NO_x emissions from power plants, the industrial
29 and residential sector, and the transportation sector play similar roles; the SO₂ emissions from
30 the industrial and residential sector have larger effects on PM_{2.5} than those from power plants
31 due to larger emissions and lower stack heights. NMVOC emissions have minor effect on
32 PM_{2.5} concentrations, mainly due to the significant underestimation of SOA in the current

1 version of CMAQ, which is also a common issue for most widely used CTMs (Robinson et al.,
2 2007).

3 The $PM_{2.5}$ sensitivities to primary $PM_{2.5}$ emissions are approximately the same at various
4 control levels. However, the $PM_{2.5}$ sensitivity to gaseous precursors increases notably when
5 more control efforts are taken, mainly attributable to transition between NH_3 -rich and
6 NH_3 -poor conditions. Specifically, a particular pollutant (SO_2 , NO_x , or NH_3), when subject to
7 larger reductions compared with others, will become the limiting factor for inorganic aerosol
8 chemistry. In January, the response of $PM_{2.5}$ to NO_x emissions is negative for relatively small
9 reductions (< 40 - 70%), but becomes positive for large reductions (> 40 - 70%). This strong
10 nonlinearity has also been confirmed by the previous studies (Zhao et al., 2013c; Dong et al.,
11 2014). Relatively small reductions of NO_x emissions lead to the increase of O_3 and HO_x
12 radical due to a NMVOC-limited regime for photochemistry, enhancing the formation of
13 sulfate (see Fig. 7). In addition, the increase of O_3 and HO_x radical also accelerates the
14 nighttime formation of N_2O_5 and HNO_3 through the $NO_2 + O_3$ reaction, thereby enhancing the
15 formation of nitrate aerosol (see Fig. 7). As an integrated effect, the $PM_{2.5}$ concentrations
16 increase with relatively small reductions of NO_x emissions. Under large reductions of NO_x ,
17 $PM_{2.5}$ concentrations decrease, resulting from the simultaneous decline of NO_2 , O_3 and HO_x
18 radical concentrations (NO_x -limited regime for photochemistry). These chemical processes
19 also explain why the reduction of NO_x emissions of a single emission sector has negative
20 effects on $PM_{2.5}$ even at large reduction ratio (see Fig. 6). Simultaneous reductions of NO_x
21 emissions from multiple sectors are essential for reducing $PM_{2.5}$ concentrations. If all
22 pollutants are controlled simultaneously, the sensitivity of $PM_{2.5}$ concentrations to emission
23 reductions also generally becomes larger with more control effort taken, especially in January
24 (see red dotted line in Fig. 5 and Fig. 6). Note that the effects of reducing individual pollutants
25 (from individual sectors) and reducing all of them together are different. In most cases the
26 combined effect is lower than the sum of individual effects, which can be explained by the
27 overlap effects of reductions in both species involved in the formation of ammonium sulfate
28 and ammonium nitrate. However, it is sometimes the other way around in January, as shown
29 in Fig. 6. As mentioned above, in January, the response of $PM_{2.5}$ to the reduction of NO_x
30 emissions from a single emission sector is negative since the emission reduction is small
31 compared with the total NO_x emissions. Therefore, when the NO_x emissions from each sector
32 are reduced individually (the bars), we sum up the negative effects. In contrast, when all

1 pollutants from all sectors are reduced simultaneously (the red dotted line), the NO_x emission
2 reduction at large ratio could have positive effect on $\text{PM}_{2.5}$ reduction. This is why the
3 combined effect sometimes exceeds the sum of individual effects in January.
4 Then, we evaluate the contribution of primary $\text{PM}_{2.5}$ and gaseous precursor (SO_2 , NO_x , and
5 NH_3) emissions from different regions to $\text{PM}_{2.5}$ concentrations based on the ERSM technique
6 (Table 3). The contributions of total primary $\text{PM}_{2.5}$ emissions (39-46% in January, and 43-46%
7 in August) are dominated by local sources (32-36% in January, and 37-43% in August). Total
8 gaseous precursor emissions in the domain contribute 25-36% and 48-50% of $\text{PM}_{2.5}$
9 concentrations in January and August, respectively. The relative importance of gaseous
10 precursor emissions from the other regions compared with local precursor emissions is
11 generally higher than that of primary $\text{PM}_{2.5}$; this trend is especially evident in August. In
12 Shanghai, the gaseous precursor emissions from Jiangsu and Zhejiang even contribute more
13 to the $\text{PM}_{2.5}$ concentration than local precursor emissions during August. In January, long
14 range transport has a significant effect on $\text{PM}_{2.5}$ concentrations (25-34% contribution) due to
15 the northerly monsoon, contrasted by the minor effect in August (7-8% contribution).

16 **3.3 Response of SO_4^{2-} and NO_3^- to precursor emissions**

17 We pay special attention to secondary inorganic aerosols (SIA) because SIA contribute 28-55%
18 of total $\text{PM}_{2.5}$ concentrations based on our simulation. Figure 7 shows the sensitivity of
19 $\text{NO}_3^-/\text{SO}_4^{2-}$ concentrations to the emissions of individual air pollutants in individual regions;
20 Fig. S6 shows the sensitivity of $\text{NO}_3^-/\text{SO}_4^{2-}$ concentrations to the emissions of individual air
21 pollutants from individual sectors. Both figures are derived from the prediction system built
22 with the ERSM technique. In January, NO_3^- concentration is most sensitive to NH_3 emissions,
23 especially local NH_3 emissions. The effect of local NO_x emissions on NO_3^- concentrations
24 changes from negative to positive when the controls of NO_x emissions become more and
25 more stringent. This pattern is similar to that of $\text{PM}_{2.5}$ described above. The NO_x emissions
26 from the industrial and residential sector and the transportation sector, when controlled
27 individually, both make negative contribution to the reduction of NO_3^- concentrations. In
28 contrast, the control of NO_x emissions from power plants often favors the reduction of NO_3^- ,
29 because power plants tend to affect the fine particles over a larger spatial scale due to their
30 higher release heights, and because the photochemistry typically changes from a
31 NMVOC-limited regime in surface metropolis areas to a NO_x -limited regime in vast rural
32 areas or the upper air (Xing et al., 2011). In August, NO_3^- concentrations are mainly affected

1 by local emissions of NH_3 and NO_x , as well as NO_x emissions in upwind regions, and NO_x
2 emissions make a much larger positive contribution to NO_3^- concentrations compared with
3 January. Factors accounting for this difference include a stronger NH_3 -rich condition for
4 inorganic aerosol chemistry (Wang et al., 2011), and a weaker NMVOC-limited (in
5 metropolis areas) or a stronger NO_x -limited (in rural areas) photochemical condition in
6 August. The contributions of NO_x emissions from power plants, the industrial and residential
7 sector, and the transportation sector are similar to each other.

8 In January, SO_4^{2-} concentrations are dominated by the changes of local SO_2 emissions,
9 followed by local NH_3 emissions. NO_x emissions have a negative effect on SO_4^{2-} due to both
10 thermodynamic (competition with SO_2 for NH_3) and photochemical effect (negatively
11 correlated with O_3 and HO_x radical). In August, SO_4^{2-} is most sensitive to local SO_2 and NH_3
12 emissions. In Shanghai, where local emissions are relatively small compared with emissions
13 in other regions, the SO_2 and NH_3 emissions from upwind regions might contribute more to
14 SO_4^{2-} concentration than local emissions. In both January and August, the SO_2 emissions of
15 the industrial and residential sector have larger effects on SO_4^{2-} concentrations than those of
16 power plants, partly due to larger emissions and lower stack heights.

17 **4 Conclusions, implications, and limitations**

18 In this study, we developed a novel Extended Response Surface Modeling technique (ERSM
19 v1.0). As an advantage over previous models or techniques, this technique could
20 characterize the nonlinear response of $\text{PM}_{2.5}$ and its chemical components to large and
21 simultaneous changes of multiple precursor emissions from multiple regions and sectors with
22 a reasonable number of model scenarios. The ERSM technique was developed starting from
23 the conventional RSM technique; it first quantifies the relationship between $\text{PM}_{2.5}$
24 concentrations and the emissions of gaseous precursors from each single region with the
25 conventional RSM technique, and then assesses the effects of inter-regional transport of $\text{PM}_{2.5}$
26 and its gaseous precursors on $\text{PM}_{2.5}$ concentrations in the target region. A particular approach
27 was implemented to improve the accuracy of the response surface when the emissions from
28 multiple regions experience quite large reductions simultaneously.

29 We applied the ERSM technique with CMAQ version 4.7.1 over the YRD region of China,
30 and mapped the concentrations of $\text{PM}_{2.5}$ and its inorganic components versus 36 control
31 variables. Using the ERSM technique, we predicted the $\text{PM}_{2.5}$ concentrations for 40
32 independent control scenarios, and compared with the corresponding CMAQ simulations. The

1 comparison results show that the ERSM predictions and CMAQ simulations agree well with
2 each other. The correlation coefficients are larger than 0.98 and 0.99, and the mean
3 normalized errors are less than 1% and 2% for January and August, respectively. We also
4 compared the 2D-isopleths of $PM_{2.5}$ concentrations in response to the changes of precursor
5 emissions derived from both the conventional RSM and the ERSM technique, and
6 demonstrated that the ERSM technique could reproduce fairly well the response of $PM_{2.5}$ to
7 continuous changes of precursor emission levels between zero and 150%.

8 Employing the ERSM technique, we identified the major sources contributing to $PM_{2.5}$ and its
9 inorganic components in the YRD region. For example, in January, $PM_{2.5}$ concentrations are
10 sensitive to the primary $PM_{2.5}$ emissions, followed by NH_3 , and relatively insensitive to NO_X
11 and SO_2 . During August, gaseous precursors make larger contributions to $PM_{2.5}$
12 concentrations than primary $PM_{2.5}$, with similar contributions from NH_3 , SO_2 , and NO_X . We
13 also characterized the nonlinearity in the response of $PM_{2.5}$ to emission changes and
14 illustrated the underlying chemical processes. For example, the sensitivity of $PM_{2.5}$ to gaseous
15 precursors increases notably when more control efforts are taken, due to the transition
16 between NH_3 -rich and NH_3 -poor conditions. In January, the response of $PM_{2.5}$ to NO_X
17 emissions is negative for relatively small reductions, but becomes positive for large
18 reductions.

19 The assessment of the response of $PM_{2.5}$ and its inorganic components to precursor emissions
20 over the YRD region has important policy implications. First, the control of primary $PM_{2.5}$
21 emissions, especially those of the industrial and residential sources, should be enhanced
22 considering their large contribution to $PM_{2.5}$ concentrations. Second, NO_X emissions need be
23 reduced substantially in order to mitigate the adverse effect on $PM_{2.5}$ concentrations at
24 relatively small reduction ratio. Third, the control of NH_3 should be implemented in
25 heavy-pollution areas in winter due to its significant effect on $PM_{2.5}$. Fourth, it is essential to
26 implement region-dependent emission reduction targets based on the above-quantified
27 interactions among regions.

28 Except for identification of major emission sources, the ERSM technique has several other
29 practical applications. First, it allows us to calculate the required emission reductions to attain
30 a certain environmental target. Specifically, we alter the emission ratios of various control
31 variables and calculate the “real-time” response of $PM_{2.5}$ concentrations with ERSM
32 repeatedly until the standard is attained. Second, ERSM can be applied to design optimal

1 control options, which could be determined through cost-effective optimization once ERSM is
2 coupled with control cost models/functions that links the emission reductions with private
3 costs.

4 The ERSM technique still has several limitations. Firstly, the technique currently does not
5 consider the variability of meteorological conditions. Secondly, although the ERSM technique
6 represents an essential improvement compared with the conventional RSM technique, it
7 usually needs over 500 emission scenarios for a medium-size problem. Future studies should
8 be done to further reduce the number of scenarios required while assuring the accuracy of the
9 response surfaces. Thirdly, the emission scenarios required to build the response surface
10 depends strictly on the experimental design (e.g., selection of geographical regions and
11 control variables). It is not necessary to recompute lots of CTM simulations if we make minor
12 revision on the experimental design. For example, if one more geographical area is added, we
13 just need to (1) add a parallel group of emission scenarios where the control variables of the
14 added geographical area change while those of the other regions remain the base-case levels,
15 and (2) recompute the emission scenarios where the control variables of all regions change
16 simultaneously. Another example, if the selected emission sectors in a specific geographical
17 area are changed, we just need to recompute the group of emission scenarios where the
18 control variables of this geographical area change while those of the other regions remain the
19 base-case levels. However, if the experimental design is significantly changed (e.g., change of
20 selected pollutants, or change of selected emission sectors in all regions), most of the CTM
21 simulations need to be recomputed. The users need to carefully design the experiment before
22 performing the CTM simulations.

23 24 25 **Code availability**

26 All codes needed to run ERSM v1.0 in MATLAB[®] are available upon the request. Any
27 potential user interested in the model should contact S. X. Wang, and any feedback on them is
28 welcome. Procedures to run the model and sources of external data files are properly
29 documented in a Manual.doc file.

30 31 **Author contribution**

1 B. Zhao, J. Xing, and S. X. Wang developed the underlying algorithms of the model. B. Zhao
2 and K. Fu developed the model code and performed the simulations. B. Zhao, K. Fu and W. J.
3 Wu conducted the model validation. B. Zhao and S. X. Wang prepared the manuscript with
4 contributions from all co-authors. J. S. Fu, C. Jang, Y. Zhu, X. Y. Dong, Y. Gao and J. M.
5 Hao provided important academic guidance.

6
7 **Acknowledgment.** This work was sponsored by National Natural Science Foundation of
8 China (21221004), Strategic Priority Research Program of the Chinese Academy of Sciences
9 (XBD05020300), and MEP's Special Funds for Research on Public Welfares (201409002,
10 201309009). The authors also appreciate the support from Collaborative Innovation Center
11 for Regional Environmental Quality of Tsinghua University.

12 13 **References**

- 14 Amann, M., Cofala, J., Gzella, A., Heyes, C., Klimont, Z., and Schopp, W.: Estimating
15 concentrations of fine particulate matter in urban background air of European cities, Interim
16 Report IR-07-001, available at <http://www.iiasa.ac.at>, International Institute for Applied
17 Systems Analysis, Laxenburg, Austria, 50, 2007.
- 18 Carlton, A. G., Bhave, P. V., Napelenok, S. L., Edney, E. D., Sarwar, G., Pinder, R. W.,
19 Pouliot, G. A., and Houyoux, M.: Model Representation of Secondary Organic Aerosol in
20 CMAQv4.7, *Environ. Sci. Technol.*, 44, 8553-8560, DOI 10.1021/Es100636q, 2010.
- 21 Carmichael, G. R., Sandu, A., and Potra, F. A.: Sensitivity analysis for atmospheric chemistry
22 models via automatic differentiation, *Atmos. Environ.*, 31, 475-489, DOI
23 10.1016/S1352-2310(96)00168-9, 1997.
- 24 Dickerson, R. R., Stedman, D. H., and Delany, A. C.: Direct Measurements of Ozone and
25 Nitrogen-Dioxide Photolysis Rates in the Troposphere, *J. Geophys. Res.-Oc. Atm.*, 87,
26 4933-4946, DOI 10.1029/Jc087ic07p04933, 1982.
- 27 Dong, X. Y., Li, J., Fu, J. S., Gao, Y., Huang, K., and Zhuang, G. S.: Inorganic aerosols
28 responses to emission changes in Yangtze River Delta, China, *Sci. Total. Environ.*, 481,
29 522-532, DOI 10.1016/j.scitotenv.2014.02.076, 2014.
- 30 Fu, J. S., Brill, E. D., and Ranjithan, S. R.: Conjunctive use of models to design cost-effective
31 ozone control strategies, *J. Air. Waste. Manage.*, 56, 800-809, 2006.
- 32 Fu, X., Wang, S. X., Zhao, B., Xing, J., Cheng, Z., Liu, H., and Hao, J. M.: Emission
33 inventory of primary pollutants and chemical speciation in 2010 for the Yangtze River
34 Delta region, China, *Atmos. Environ.*, 70, 39-50, DOI 10.1016/j.atmosenv.2012.12.034,
35 2013.
- 36 Guenther, A., Karl, T., Harley, P., Wiedinmyer, C., Palmer, P. I., and Geron, C.: Estimates of
37 global terrestrial isoprene emissions using MEGAN (Model of Emissions of Gases and
38 Aerosols from Nature), *Atmos. Chem. Phys.*, 6, 3181-3210, 2006.
- 39 Hakami, A., Odman, M. T., and Russell, A. G.: High-order, direct sensitivity analysis of
40 multidimensional air quality models, *Environ. Sci. Technol.*, 37, 2442-2452, DOI
41 10.1021/Es020677h, 2003.

1 Hakami, A., Seinfeld, J. H., Chai, T. F., Tang, Y. H., Carmichael, G. R., and Sandu, A.:
2 Adjoint sensitivity analysis of ozone nonattainment over the continental United States,
3 *Environ. Sci. Technol.*, 40, 3855-3864, DOI 10.1021/Es052135g, 2006.

4 Heyes, C., Schopp, W., Amann, M., and Unger, S.: A reduced-form model to predict
5 long-term ozone concentrations in Europe, Interim Report WP-96-12, available at
6 <http://www.iiasa.ac.at>, International Institute for Applied Systems Analysis, Laxenburg,
7 Austria, 58, 1996.

8 Hwang, J. T., Dougherty, E. P., Rabitz, S., and Rabitz, H.: Greens Function Method of
9 Sensitivity Analysis in Chemical-Kinetics, *J. Chem. Phys.*, 69, 5180-5191, DOI
10 10.1063/1.436465, 1978.

11 Iman, R. L., Davenport, J. M., and Zeigler, D. K.: Latin Hypercube Sampling (Program User's
12 Guide), Sandia National Laboratories, Albuquerque, NM, U.S. Technical Report
13 SAND79-1473, 78, 1980.

14 Milford, J. B., Russell, A. G., and Mcrae, G. J.: A New Approach to Photochemical
15 Pollution-Control - Implications of Spatial Patterns in Pollutant Responses to Reductions in
16 Nitrogen-Oxides and Reactive Organic Gas Emissions, *Environ. Sci. Technol.*, 23,
17 1290-1301, DOI 10.1021/Es00068a017, 1989.

18 Nel, A.: Air pollution-related illness: Effects of particles, *Science*, 308, 804-806, DOI
19 10.1126/science.1108752, 2005.

20 Robinson, A. L., Donahue, N. M., Shrivastava, M. K., Weitkamp, E. A., Sage, A. M.,
21 Grieshop, A. P., Lane, T. E., Pierce, J. R., and Pandis, S. N.: Rethinking organic aerosols:
22 Semivolatile emissions and photochemical aging, *Science*, 315, 1259-1262, DOI
23 10.1126/science.1133061, 2007.

24 Russell, A., Milford, J., Bergin, M. S., Mcbride, S., Mcnair, L., Yang, Y., Stockwell, W. R.,
25 and Croes, B.: Urban Ozone Control and Atmospheric Reactivity of Organic Gases,
26 *Science*, 269, 491-495, DOI 10.1126/science.269.5223.491, 1995.

27 Sandu, A., Daescu, D. N., Carmichael, G. R., and Chai, T. F.: Adjoint sensitivity analysis of
28 regional air quality models, *J. Comput. Phys.*, 204, 222-252, DOI
29 10.1016/j.jcp.2004.10.011, 2005.

30 Sandu, A., and Zhang, L.: Discrete second order adjoints in atmospheric chemical transport
31 modeling, *J. Comput. Phys.*, 227, 5949-5983, DOI 10.1016/j.jcp.2008.02.011, 2008.

32 Santner, T. J., Williams, B. J., and Notz, W.: The Design and Analysis of Computer
33 Experiments, Springer Verlag, New York, U.S., 283 pp., 2003.

34 Simon, H., Baker, K. R., Akhtar, F., Napelenok, S. L., Possiel, N., Wells, B., and Timin, B.:
35 A Direct Sensitivity Approach to Predict Hourly Ozone Resulting from Compliance with
36 the National Ambient Air Quality Standard, *Environ. Sci. Technol.*, 47, 2304-2313, DOI
37 10.1021/Es303674e, 2013.

38 Stocker, T. F., Qin, D., Plattner, G.-K., Tignor, M., Allen, S. K., Boschung, J., Nauels, A., Xia,
39 Y., Bex, V., and Midgley, P. M.: Climate Change 2013: The Physical Science Basis.
40 Contribution of Working Group I to the Fifth Assessment Report of the Intergovernmental
41 Panel on Climate Change, Cambridge University Press, Cambridge, United Kingdom and
42 New York, NY, USA, 1535 pp., 2013.

43 U.S. Environmental Protection Agency: Technical support document for the proposed PM
44 NAAQS rule: Response Surface Modeling, Office of Air Quality Planning and Standards,
45 U.S. Environmental Protection Agency, Research Triangle Park, NC, U.S., 48, 2006a.

46 U.S. Environmental Protection Agency: Technical support document for the proposed mobile
47 source air toxics rule: ozone modeling, Office of Air Quality Planning and Standards, U.S.
48 Environmental Protection Agency, Research Triangle Park, NC, U.S., 49, 2006b.

1 Wang, L. H., and Milford, J. B.: Reliability of optimal control strategies for photochemical air
2 pollution, *Environ. Sci. Technol.*, 35, 1173-1180, DOI 10.1021/Es001358y, 2001.

3 Wang, S. X., Xing, J., Jang, C. R., Zhu, Y., Fu, J. S., and Hao, J. M.: Impact assessment of
4 ammonia emissions on inorganic aerosols in east China using response surface modeling
5 technique, *Environ. Sci. Technol.*, 45, 9293-9300, DOI 10.1021/Es2022347, 2011.

6 Wang, S. X., and Hao, J. M.: Air quality management in China: Issues, challenges, and
7 options, *J. Environ. Sci-China.*, 24, 2-13, DOI 10.1016/S1001-0742(11)60724-9, 2012.

8 Wang, S. X., Zhao, B., Cai, S. Y., Klimont, Z., Nielsen, C., McElroy, M. B., Morikawa, T.,
9 Woo, J. H., Kim, Y., Fu, X., Xu, J. Y., Hao, J. M., and He, K. B.: Emission trends and
10 mitigation options for air pollutants in East Asia, *Atmos. Chem. Phys. Discuss.*, 14,
11 2601-2674, DOI 10.5194/acpd-14-2601-2014, 2014.

12 Xing, J.: Study on the nonlinear responses of air quality to primary pollutant emissions,
13 Doctor thesis, School of Environment, Tsinghua University, Beijing, China, 138 pp., 2011
14 (in Chinese).

15 Xing, J., Wang, S. X., Jang, C., Zhu, Y., and Hao, J. M.: Nonlinear response of ozone to
16 precursor emission changes in China: a modeling study using response surface
17 methodology, *Atmos. Chem. Phys.*, 11, 5027-5044, DOI 10.5194/acp-11-5027-2011, 2011.

18 Yang, Y. J., Wilkinson, J. G., and Russell, A. G.: Fast, direct sensitivity analysis of
19 multidimensional photochemical models, *Environ. Sci. Technol.*, 31, 2859-2868, DOI
20 10.1021/Es970117w, 1997.

21 Yarwood, G., Emery, C., Jung, J., Nopmongcol, U., and Sakulyanontvittaya, T.: A method to
22 represent ozone response to large changes in precursor emissions using high-order
23 sensitivity analysis in photochemical models, *Geosci. Model. Dev.*, 6, 1601-1608, DOI
24 10.5194/gmd-6-1601-2013, 2013.

25 Zhang, Q., Streets, D. G., Carmichael, G. R., He, K. B., Huo, H., Kannari, A., Klimont, Z.,
26 Park, I. S., Reddy, S., Fu, J. S., Chen, D., Duan, L., Lei, Y., Wang, L. T., and Yao, Z. L.:
27 Asian emissions in 2006 for the NASA INTEX-B mission, *Atmos. Chem. Phys.*, 9,
28 5131-5153, 2009a.

29 Zhang, X. Y., Wang, Y. Q., Niu, T., Zhang, X. C., Gong, S. L., Zhang, Y. M., and Sun, J. Y.:
30 Atmospheric aerosol compositions in China: spatial/temporal variability, chemical
31 signature, regional haze distribution and comparisons with global aerosols, *Atmos. Chem.*
32 *Phys.*, 12, 779-799, DOI 10.5194/acp-12-779-2012, 2012.

33 Zhang, Y., Wen, X. Y., Wang, K., Vijayaraghavan, K., and Jacobson, M. Z.: Probing into
34 regional O₃ and particulate matter pollution in the United States: 2. An examination of
35 formation mechanisms through a process analysis technique and sensitivity study, *J.*
36 *Geophys. Res-Atmos.*, 114, DOI 10.1029/2009jd011900, 2009b.

37 Zhao, B., Wang, S. X., Dong, X. Y., Wang, J. D., Duan, L., Fu, X., Hao, J. M., and Fu, J.:
38 Environmental effects of the recent emission changes in China: implications for particulate
39 matter pollution and soil acidification, *Environ. Res. Lett.*, 8, DOI
40 10.1088/1748-9326/8/2/024031, 2013a.

41 Zhao, B., Wang, S. X., Liu, H., Xu, J. Y., Fu, K., Klimont, Z., Hao, J. M., He, K. B., Cofala,
42 J., and Amann, M.: NO_x emissions in China: historical trends and future perspectives,
43 *Atmos. Chem. Phys.*, 13, 9869-9897, DOI 10.5194/acp-13-9869-2013, 2013b.

44 Zhao, B., Wang, S. X., Wang, J. D., Fu, J. S., Liu, T. H., Xu, J. Y., Fu, X., and Hao, J. M.:
45 Impact of national NO_x and SO₂ control policies on particulate matter pollution in China,
46 *Atmos. Environ.*, 77, 453-463, DOI 10.1016/j.atmosenv.2013.05.012, 2013c.

47
48

1 Tables and figures

2 Table 1. Description of the RSM/ERSM prediction systems developed in this study.

method	variable number	control variables	scenario number	scenario details
conventional RSM technique	5	total emissions of NO _x , SO ₂ , NH ₃ , NMVOC, and PM _{2.5}	101	1 CMAQ base case; 100 ^a scenarios generated by applying LHS method for the 5 variables.
ERSM technique	36	9 variables in each of the 4 regions, including 6 gaseous variables, i.e., (1) NO _x /Power plants (2) NO _x /Industrial and residential (3) NO _x /Transportation (4) SO ₂ /Power plants (5) SO ₂ /Industrial and Residential (6) NH ₃ /All sectors, and 3 primary PM _{2.5} variables, i.e., (7) PM _{2.5} /Power plants (8) PM _{2.5} /Industrial and residential (9) PM _{2.5} /Transportation.	663	1 CMAQ base case; 600 scenarios, including 150 ^a scenarios generated by applying LHS method for the gaseous control variables in Shanghai, 150 scenarios generated in the same way for Jiangsu, 150 scenarios for Zhejiang, 150 scenarios for Others; 50 ^a scenarios generated by applying LHS method for the total NO _x , SO ₂ , and NH ₃ emissions; 12 scenarios where one primary PM _{2.5} control variable is set to 0.25 for each scenario.

3 ^a 100, 150 and 50 scenarios are needed for the response surfaces for 5, 6 and 3 variables, respectively (Xing et
4 al., 2011; Wang et al., 2011).

5

6 Table 2. Comparison of PM_{2.5} concentrations predicted by the ERSM technique with
7 out-of-sample CMAQ simulations.

	January			August		
	Shanghai	Jiangsu	Zhejiang	Shanghai	Jiangsu	Zhejiang
Correlation coefficient	0.989	0.980	0.987	0.995	0.997	0.994
Mean Normalized Error (MNE)	1.0%	0.7%	0.9%	0.8%	0.5%	1.7%
Maximum Normalized Error (NE)	4.5%	3.0%	5.2%	10.2%	7.7%	9.6%
95% percentile of NEs	2.8%	2.7%	3.5%	3.0%	1.6%	3.1%
MNE (case 33-36)	0.0%	0.0%	0.0%	0.1%	0.1%	0.1%
Maximum NE (case 33-36)	0.1%	0.1%	0.1%	0.1%	0.1%	0.2%

8

1

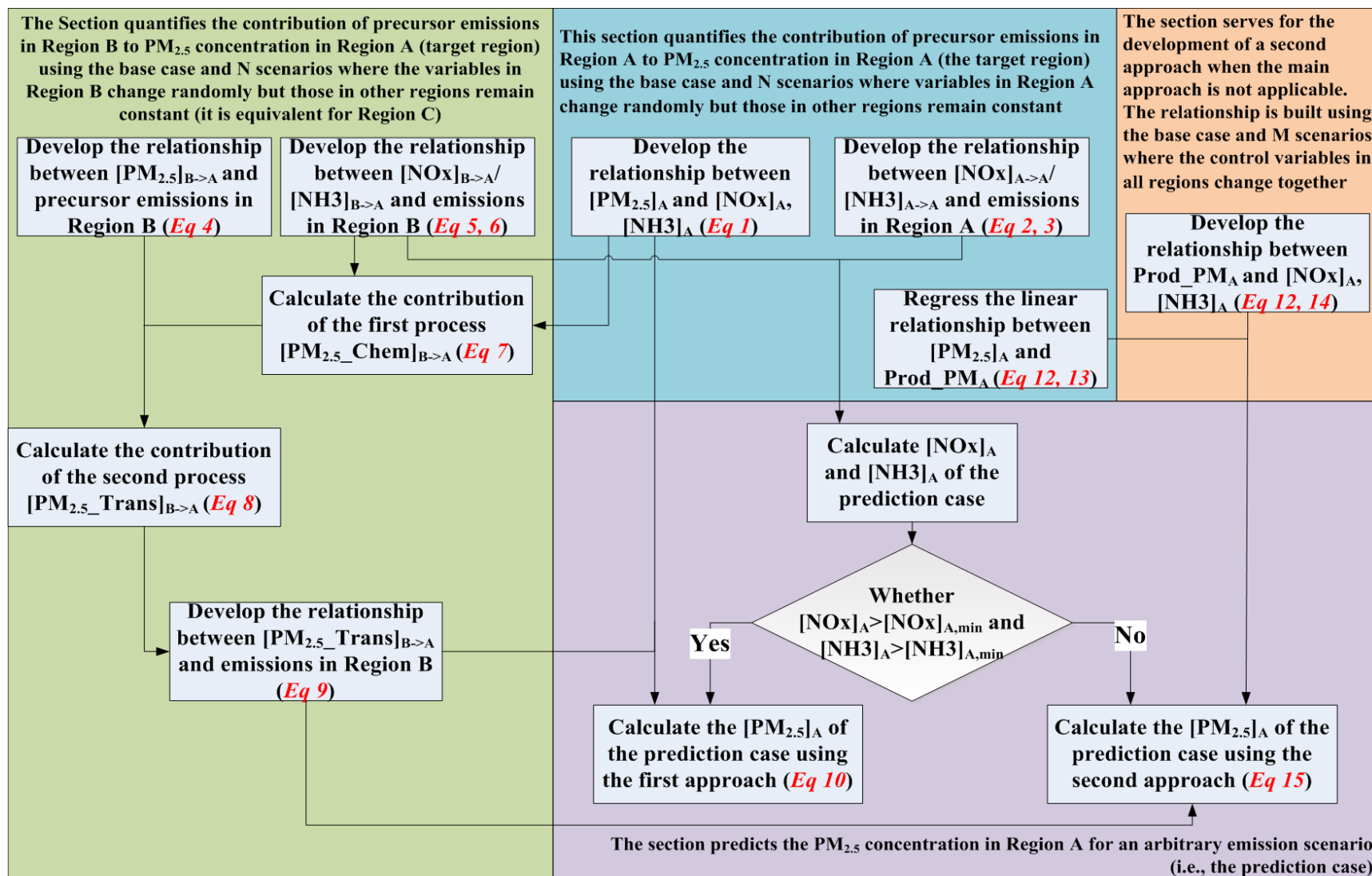
2 Table 3. Contribution of primary PM_{2.5} and gaseous precursor (NO_x, SO₂, NH₃) emissions

3 from individual regions to PM_{2.5} concentrations.

	January			August		
	Shanghai	Jiangsu	Zhejiang	Shanghai	Jiangsu	Zhejiang
Emissions of Primary PM _{2.5} in Shanghai	35.5%	1.1%	1.3%	36.9%	1.0%	0.4%
Emissions of Primary PM _{2.5} in Jiangsu	5.6%	35.0%	4.1%	2.2%	37.5%	0.9%
Emissions of Primary PM _{2.5} in Zhejiang	1.9%	2.3%	32.2%	4.3%	2.5%	42.8%
Emissions of Primary PM _{2.5} in Others	2.9%	2.9%	1.7%	2.0%	1.9%	1.5%
Emissions of Primary PM _{2.5} in four regions	46.0%	41.2%	39.4%	45.4%	42.9%	45.7%
Emissions of NO _x , SO ₂ , and NH ₃ in Shanghai	11.3%	0.2%	1.0%	18.9%	1.8%	2.5%
Emissions of NO _x , SO ₂ , and NH ₃ in Jiangsu	3.3%	11.7%	3.9%	5.2%	30.1%	4.3%
Emissions of NO _x , SO ₂ , and NH ₃ in Zhejiang	2.7%	4.3%	20.9%	18.3%	12.6%	36.3%
Emissions of NO _x , SO ₂ , and NH ₃ in Others	1.7%	2.4%	2.8%	5.7%	4.6%	7.2%
Emissions of NO _x , SO ₂ , and NH ₃ in four regions	25.2%	24.9%	35.7%	48.3%	50.4%	47.7%
Emissions of Primary PM _{2.5} in the outer domain	7.4%	9.1%	6.3%	0.7%	0.8%	1.6%
Emissions of NO _x , SO ₂ , and NH ₃ in outer domain	20.6%	24.5%	19.1%	6.6%	7.1%	6.1%

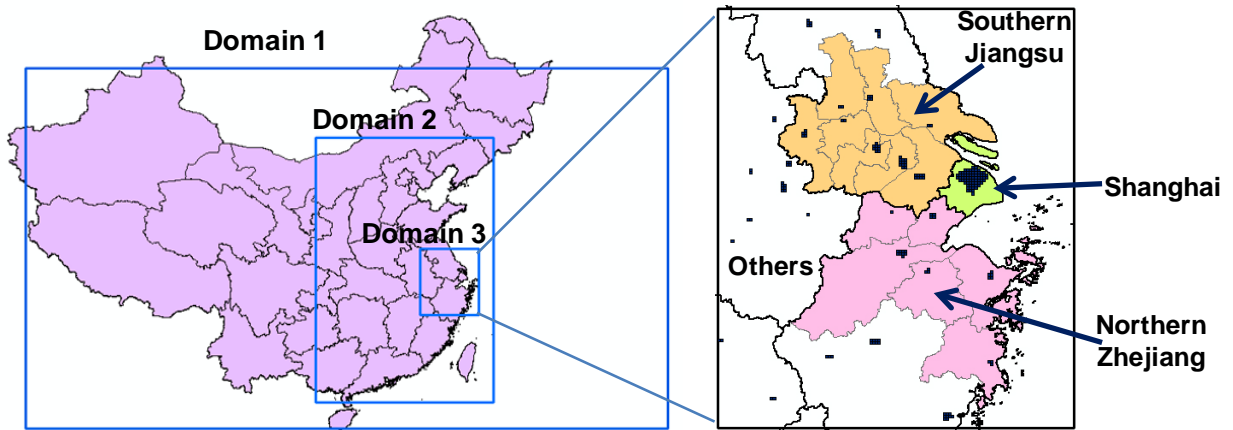
4

5



1
 2 Figure 1. A flowchart illustrating the ERSM technique using the simplified case described in Sect. 2.1. Different background colors
 3 represent the procedures conducted using different groups of emission scenarios, as indicated on the top/bottom of the colored areas.

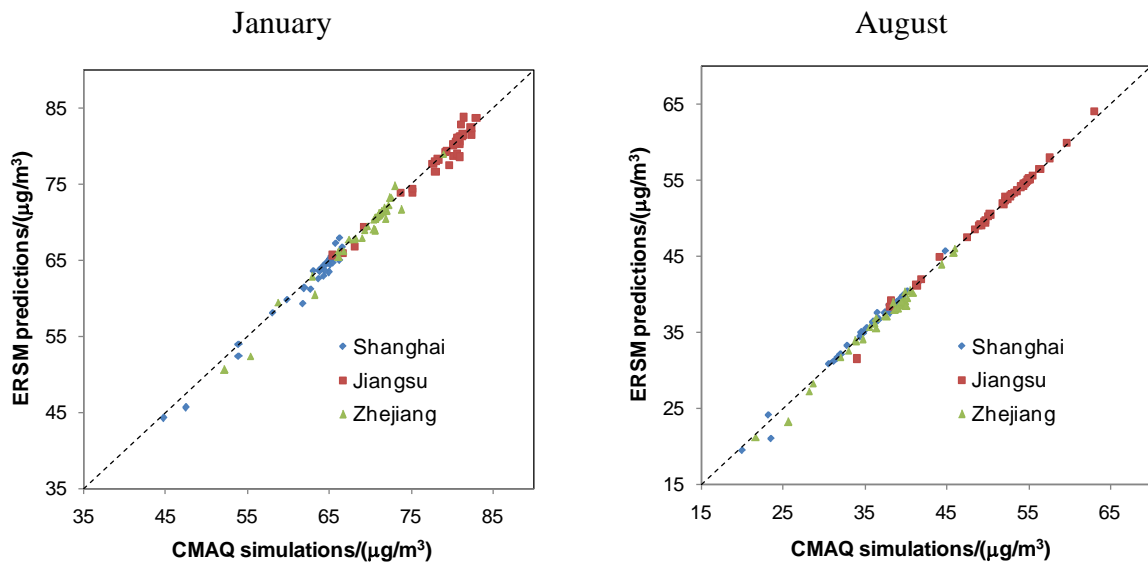
1



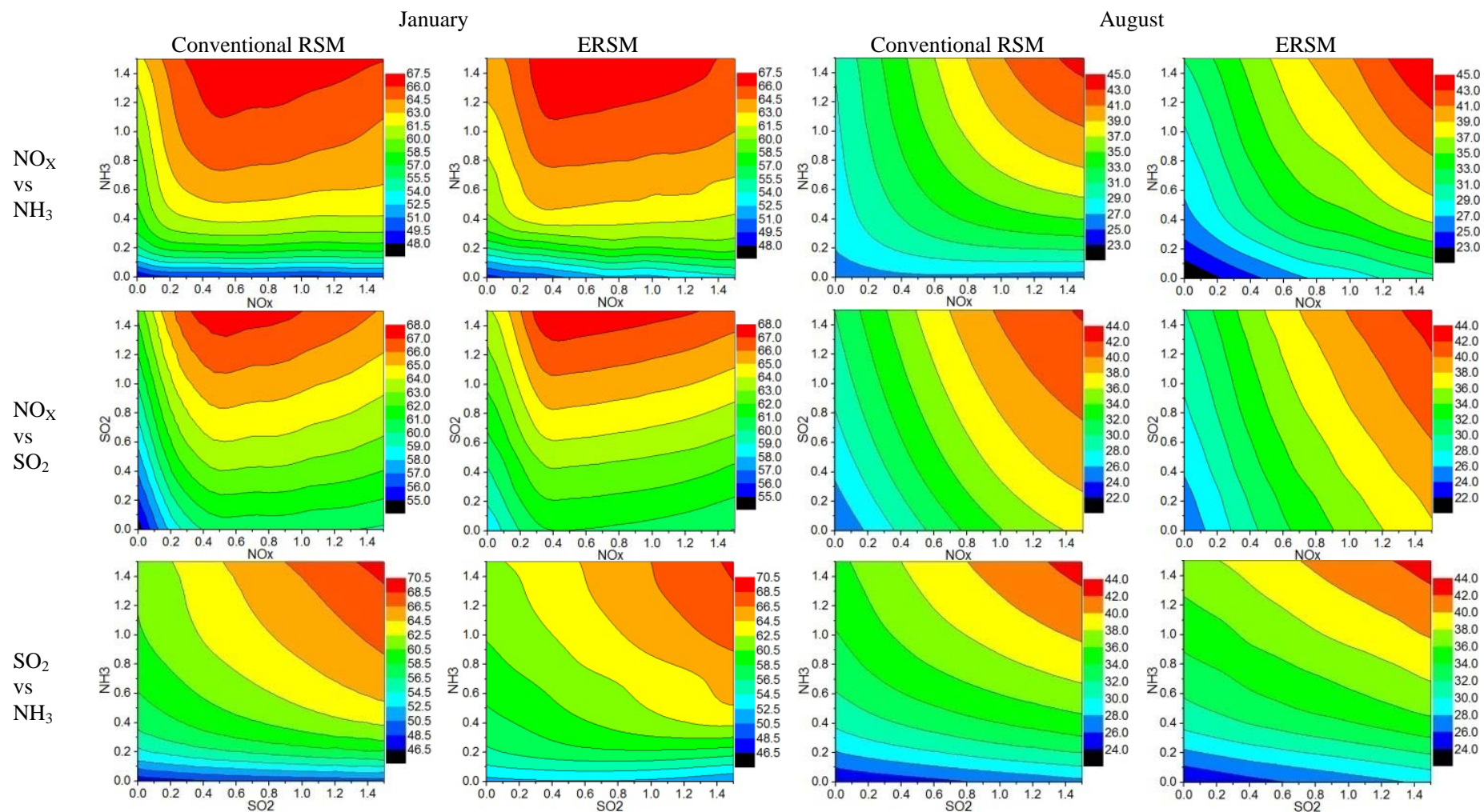
2

3 Figure 2. Triple nesting domains used in CMAQ simulation (left) and the definition of four
4 regions in the innermost domain, denoted by different colors (right). The black lines in the left
5 figure represent provincial boundaries; the thick black lines and the thin grey lines in the right
6 figure represent the provincial boundaries and city boundaries, respectively. The dark blue
7 grids in the right figure represent the urban areas of major cities.

8

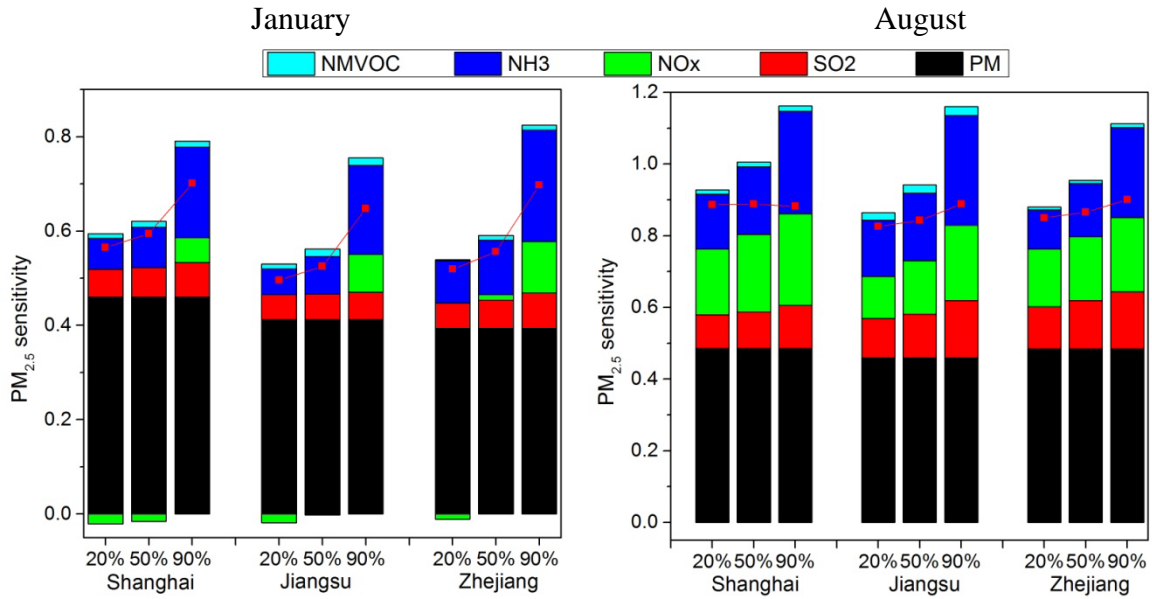


9 Figure 3. Comparison of $PM_{2.5}$ concentrations predicted by the ERSM technique with
10 out-of-sample CMAQ simulations. The dashed line is the one-to-one line indicating perfect
11 agreement.

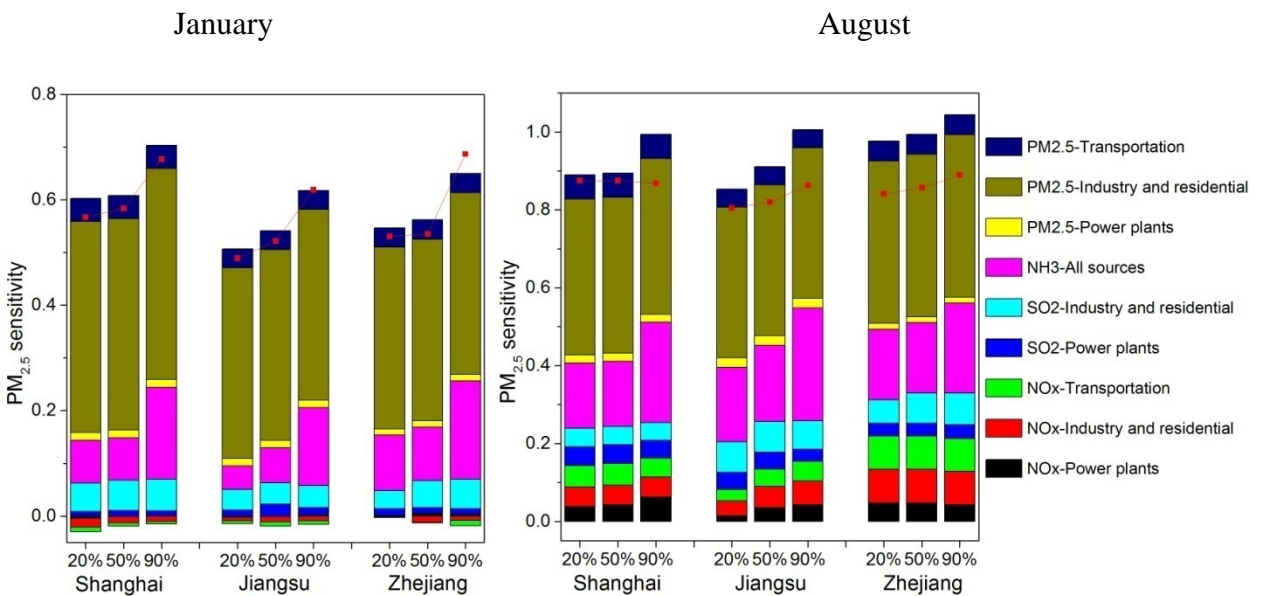


1 Figure 4. Comparison of the 2-D isopleths of $PM_{2.5}$ concentrations in Shanghai in response to the simultaneous changes of precursor
 2 emissions in all regions derived from the conventional RSM technique and the ERSM technique. The X- and Y-axis shows the emission
 3 ratio, defined as the ratios of the changed emissions to the emissions in the base case. The different colors represent different $PM_{2.5}$
 4 concentrations (unit: $\mu g m^{-3}$).

1

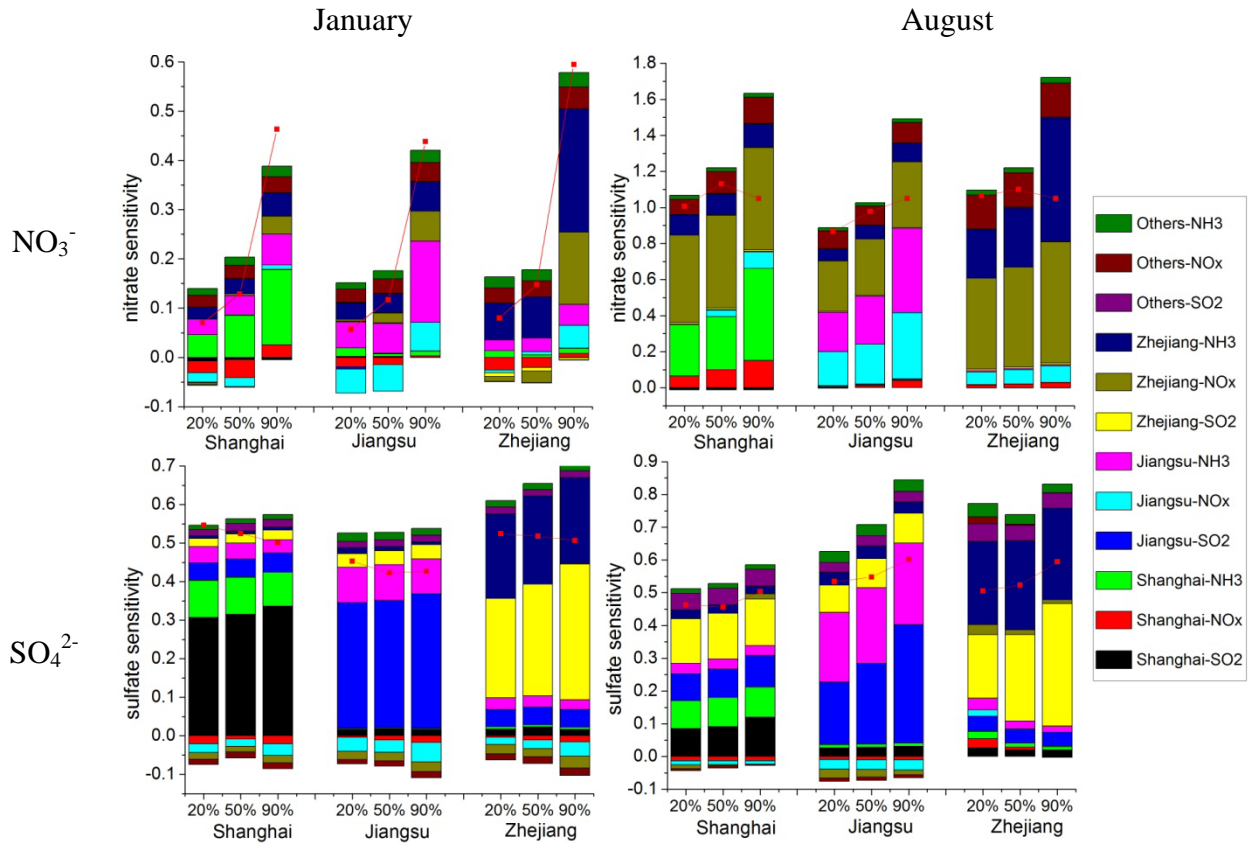


2 Figure 5. Sensitivity of PM_{2.5} concentrations to the stepped control of individual air pollutants.
 3 The X-axis shows the reduction ratio (= 1 – emission ratio). The Y-axis shows PM_{2.5}
 4 sensitivity, which is defined as the change ratio of concentration divided by the reduction
 5 ratio of emissions. The colored bars denote the PM_{2.5} sensitivities when a particular pollutant
 6 is controlled while the others stay the same as the base case; the red dotted line denotes the
 7 PM_{2.5} sensitivity when all emission sources are controlled simultaneously.
 8



9 Figure 6. Sensitivity of PM_{2.5} concentrations to the stepped control of individual air pollutants
 10 from individual sectors. The X-axis shows the reduction ratio (= 1 – emission ratio). The
 11 Y-axis shows PM_{2.5} sensitivity, which is defined as the change ratio of concentration divided
 12 by the reduction ratio of emissions. The colored bars denote the PM_{2.5} sensitivities when a

1 particular emission source is controlled while the others stay the same as the base case; the
 2 red dotted line denotes the $PM_{2.5}$ sensitivity when all emission sources are controlled
 3 simultaneously.
 4



5 Figure 7. Sensitivity of NO_3^- and SO_4^{2-} concentrations to the stepped control of individual air
 6 pollutants in individual regions. The X-axis shows the reduction ratio (= 1 – emission ratio).
 7 The Y-axis shows NO_3^-/SO_4^{2-} sensitivity, which is defined as the change ratio of NO_3^-/SO_4^{2-}
 8 concentration divided by the reduction ratio of emissions. The colored bars denote the
 9 NO_3^-/SO_4^{2-} sensitivities when a particular emission source is controlled while the others stay
 10 the same as the base case; the red dotted line denotes the NO_3^-/SO_4^{2-} sensitivity when all
 11 emission sources are controlled simultaneously.